Proceedings of the International Conference on Isochronous Cyclotrons, Gatlinburg, Tennessee, 1966

PHASE SPACE DENSITY STUDIES ON CYCLOTRON ION SOURCES*

M. L. Mallory and H. G. Blosser
Michigan State University
East Lansing, Michigan

Abstract. Using the MSU source testing facility, the phase space density of a cyclotron-type ion source has been computed from axial and radial emittance-area measurements at a variety of arc conditions and for a number of source geometries. Studies to date have all employed a 1.5 x 9 mm source output slit. Arc currents have been varied from 0.5 to 5 amps. Geometrical variations have thus far been principally concerned with explorations of the focusing effects of various source face shapes. Both axial and radial emittance areas from a normal flat source are found to have a considerable admixture of coherent motion which results in inefficient use of aperture and also, in combination with non-linear fields, can lead to an effective dilution of the phase space density. Moderate recessing of the source contributes a focusing force in both r and z and makes the phase space volume much more compact.

The effects of plasma boundary and space charge are evidenced in the axial measurements. The axial plasma boundary is found to be concave, with the results that ions emitted from the top and bottom of the ion source slit are focused toward the median plane. Space charge effects are clearly discernable; the axial width of the beam linearly increases as a function of total beam current. In the radial emittance area measurements, an asymmetry of the radial position of maximum current which varied as arc current was found and traced to a shifting plasma boundary which was the result of a strain displacement of the ion source filament.

Introduction

B. L. Cohen has studied the relationship between the best resolution obtainable with an accelerator magnetic analyzing system and the rate at which reaction-product particles are received at the detector[1]. The results of the study show that the beam from the accelerator, in all ordinary cases, more than fills the phase-space volume accepted by the analyzing system and that the optimum resolution in this case depends on the phase space density of the accelerator beam to the 1/6.5 power. The extracted phase space density of an accelerator is linearly proportional to the phase space density of the ion source. Hence increasing the phase space density of the cyclotron ion source will have the desirable result of improving the resolution of any nuclear reaction experiment.

Let the coordinates r and z designate displacements at right angles to the principle direction of motion of a beam of particles, and p_r and p_z the corresponding conjugate momenta. The phase space density of some small element of the beam is then the current (particle per unit time) in the element divided by the product of the spreads in energy, in r, p_r, z and p_z of the element.

$$D = \frac{I}{(\Delta r)(\Delta p_r)(\Delta z)(\Delta p_z)(\Delta E)} \qquad (1)$$

In the apparatus used in this experiment the energy spread (ΔE) was primarily due to the voltage ripple of the - 30 kV dc "dee" power supply and this was found to be very small resulting in a negligible coupling effect of ΔE on the other functions. Consequently, the Δr, Δp_r, Δz, Δp_z projection (ρ) of the total phase space density is considered here.

$$\rho = \frac{I}{(\Delta r)(\Delta p_r)(\Delta z)(\Delta p_z)} . \qquad (2)$$

In actual practice, the function which is usually calculated is not ρ but the luminosity L.

$$L = \frac{I}{A_r A_z} \qquad (3)$$

where A_r is the radial emittance area and is defined as the product of the radial beam spread Δr and the radial angular divergence $\Delta\alpha_r$ ($\Delta\alpha_r \approx \Delta p_r/p$ for small angles) for a given current I (p is the momentum).

$$A_r(I) = (\Delta r)(\Delta\alpha_r) = \frac{(\Delta r)(\Delta p_r)}{p} \qquad (4)$$

Likewise, A_z is the axial emittance area and is defined as the product of the axial spread Δz and the axial angular divergence $\Delta\alpha_z$ ($\Delta\alpha_z \approx \Delta p_z/p$ for small angles) for a given beam current.

$$A_z(I) = (\Delta z)(\Delta\alpha_z) = \frac{(\Delta z)(\Delta p_z)}{p} . \qquad (5)$$

The luminosity is then related to ρ by

$$L = p^2\rho . \qquad (6)$$

The problem of finding L can be reduced to measuring A_r and A_z separately (but for equal current) if no coupling exists between Δr, Δp_r and Δz, Δp_z. This is the case encountered in a uniform magnetic field and considerable design effort was made to ensure that the cyclotron ion source operated in such a field in the test facility. Certain experimental parameters were maintained constant throughout this series of measurements, namely, magnetic field (4.2 kG), dee voltage (- 30 kV dc), gas flow (1.5 cc/min. of H_2), and arc voltage (100 volts). Geometrical variations of the ion source chimney are illustrated in Fig. 1. They are face angles of 0°, 10° and 20° and barrel diameters of 0.500"(S) and 0.720"(L).

Axial Emittance Area Measurements and Results

In measuring the axial emittance area, the beam first illuminates an adjustable horizontal aperture which determines an axial beam height. Secondly, at some point further along the beam

 Reprinted from IEEE Transactions on Nuclear Science NS-13 (4), Aug 1966

trajectory, the axial angular divergence is determined by measuring the beam spread with a differential-current probe. Figure 2 shows the locations of the various probes for the axial measurement. The dotted line indicates a beam trajectory.

Figure 3 is the axial emittance area for a 0° chimney face angle at 1 amp arc current. The emittance area is 278 mm-mrad for a current of 4.24 mA. The dashed lines are density contours obtained for 87.5% and 77.0% of the total beam current and are 126 and 90 mm-mrad, respectively. Tables I and II are the axial emittance area results for different chimney configurations at 1 and 5 amps arc current, respectively.

Figure 4 is the axial emittance area of 0°, 10° and 20° chimneys at 1 amp arc current. The focusing effect of the chimney face angle is evidenced by the rotation of the axial emittance area about zero momentum, i.e., for a 0° chimney the ions are defocused while for a 20° chimney the ions are focused.

Radial Emittance Area Measurements and Results

The measurements of the radial emittance area are quite similar to the axial measurements. However, in the radial case there are certain positions where it is more advantageous to locate the radial momentum probe and radial width probe due to magnetic focusing. The best position to locate the momentum slit is at the 90° beam position where at 90° the maximum radial beam width is obtained for a given angular divergence. The best positions for the radial width probe are at beam positions of 0° and 180°; the location at 180° beam position was chosen since it is impossible to locate a probe at 0° due to high voltage problems.

The radial emittance area measured at 180° beam position is in the shape of a horseshoe and this is the result of a focusing aberration due to ions starting with different angular divergence. In fact, this aberration was used in experimentally locating the final radial probe position. This aberration, of course, does not affect the measured value of the radial emittance area. Figure 5 is the radial emittance area for a 0° chimney face angle at 1 amp arc current. The area is 370 mm-mrad for a current of 4.24 mA. The dashed lines are density contours obtained for 90% and 70% of the total beam current and the areas are 206 and 131 mm-mrad, respectively. Tables III and IV are the radial emittance area results for different chimney configurations at 1 and 5 amps arc currents.

Luminosity

In the luminosity calculations, the beam current must be known accurately for the corresponding radial and axial emittance areas. The differential probe used in the emittance measurements gave an artificially high current reading due to secondary electron loss. To determine the detection efficiency for the differential probe, a series of measurements were made with an integral probe. The integral probe had previously been checked for secondary electron loss by applying a potential to the probe in a Faraday-cup arrangement. The emittance data in combination with the current calibration then allows evaluation of the luminosity.

Figure 6 is the luminosity calculated for the 10° chimney for different arc current values and indicates that the luminosity increases approximately linearly with arc current. Table V is the luminosity for different chimneys at 1 and 5 amps arc currents and for ~ 85% beam current. Comparison of chimney barrel sizes indicates that luminosity is larger for the smaller diameters. As a function of chimney face angle the luminosity is largest at 0°, approaches a minimum at 10° and then starts to increase again at 20°.

Livingston and Jones[2] have found that the position of the plasma column and the thickness of the chimney at the slit causes large variations in output current. Variation of the plasma column position and chimney width for the different chimney configurations used in this experiment may account for the differences in measured luminosities. These factors will be investigated in later experiments.

The best source of data for estimation of the luminosity of a cyclotron ion source is from a detailed study of the Canberra cyclotron central region done by W. I. B. Smith[3]. Smith inserted a series of slits at different positions and adjusted the areas of the slits to allow passage of the beam. Blosser and Gordon[4] estimated the luminosity from the above data and found L(dc, 250 keV) = 39 A/cm^{2}sr. Applying the energy correction factor give L(dc, 30 keV) = 4.68 A/cm^{2}sr. Comparison of the above results with a typical value of Table V shows a factor of 10 larger for the measured luminosity.

Axial Plasma Boundary

The focusing peaks observed at the top and bottom of the axial emittance area are an interesting phenomenon which we believe to be due to a concave plasma boundary at the ends of the source slit. The left side of Fig. 7 is a cross section of the chimney showing such a plasma curvature at the chimney slit. The arrows represent ion trajectories and indicate that ions emitted at the top and bottom of the chimney slit are focused toward the median plane.

The right side of Fig. 7 shows a similar plasma boundary for a special chimney with a 0.031" diameter tantalum wire inserted in the center of the chimney slit. Insertion of the wire causes the plasma to form two concave surfaces. The axial emittance area is now divided into two sections, each section having two focusing peaks. Figure 8 is the measured axial emittance area with the wire inserted in the chimney and shows two emittance areas, each with focusing peaks in accord with expectation.

Space Charge Effects

Space charge effects are evidenced by an axial expansion of the beam at the 180° position which is a function of total current. Figure 9 gives the height at 180° versus total current and indicates that axial height is approximately linear with total current for a given chimney angle. This agrees with an equation derived by MacKenzie[5], (his approximation of zero focusing is excellent for our apparatus):

$$I(\text{e.s.u.}) = \frac{h}{2} \frac{\phi}{(2\pi\omega)^3} \left(\frac{e}{m}\right)^2 \frac{V^3}{r_m^4}, \qquad (7)$$

where I is the current arriving at a height h, V is the voltage per turn, ω the angular frequency, ϕ a fixed phase spread, and r_m is the radius at which magnetic focusing occurs. The effects of electric field focusing is evidenced by a shift of the curves in Fig. 9 that occurs between the 10° and 20° chimneys. The obvious important result of Fig. 9 is that shaping of the chimney face angle can be used to give an electric focusing force.

Radial Emittance Asymmetry

An asymmetry was detected in the radial emittance area measurements as a function of arc current and this was traced to a strain displacement of the ion source filament which caused a radial plasma boundary shift. Figure 10 is the radial beam spread measured at 90° position for 1 and 5 amps arc currents for different radial portions of the beam directly behind the puller. At 1 amp arc current (curve (a) of Fig. 10), the peak containing the maximum current is at the central radial position of the beam. At 5 amps arc current (curve (b) of Fig. 9) the peak with maximum current has shifted from the central position to the right. Curves (c) and (d) of Fig. 10 shows measurements made at 1 and 5 amps arc currents with a chimney having its slit moved 0.010" in the radial direction of the plasma shift. In curve (c) the maximum current peak for 1 amp is no longer located at the central beam position but has shifted to the left. In curve (d) the maximum current peak for 5 amps is now located at the central radial position. The stain displacement of the ion source filament is the result of the interaction of filament current and magnetic field. Curve (e) of Fig. 10 is the result obtained at 5 amps arc current with the direction of filament current reversed. The 5 amps maximum current peak has now shifted to the left (compared with curve (b)) of the central position of the beam. To minimize the radial asymmetry the alignment of filament with slit should be rotated by 90°.

Conclusions

The best design of the ion source chimney has not been determined. Indications are that luminosity is larger for small chimney barrel. Measurements at chimney face angles larger than 20° are needed to determine the correct angle. These and other ion source measurements are being planned.

References

1. B. L. Cohen, Rev. Sci. Instr. 33, 85 (1962).

2. R. S. Livingston and R. J. Jones, Rev. Sci. Instr. 25, 552 (1954).

3. W. I. B. Smith, Sector Focused Cyclotrons, NAS-NRC pub. 656, 183 (1959).

4. H. G. Blosser and M. M. Gordon, Nucl. Instr. & Methods 13, 101 (1961).

5. K. R. MacKenzie, Nucl. Instr. & Methods 31, 139 (1964).

* Work supported by National Science Foundation.

****

TABLE I: AXIAL EMITTANCE AREA

Arc Current = 1 amp
Energy = 30 keV

Chimney Type*	Emittance Area for 100% Current		Emittance Area for ~85% Current	
	Area mm-mrad	Current mA	Area mm-mrad	% Current
0° L	278	4.24	126	88
0° S	279	3.22	114	89
10° L	271	1.67	92	80
10° S	256	1.93	95	82
20° L	225	1.25	87	80

TABLE II: AXIAL EMITTANCE AREA

Arc Current = 5 amps
Energy = 30 keV

Chimney Type*	Emittance Area for 100% Current		Emittance Area for ~85% Current	
	Area mm-mrad	Current mA	Area mm-mrad	% Current
0° L	379	9.88	151	85
0° S	390	12.74	166	86
10° L	286	6.06	127	84
10° S	278	7.99	122	85
20° L	299	5.55	120	83

* Degrees are the amount of recesses of chimney face. S means barrel diameter of 0.500"; L means barrel diameter of 0.720".

TABLE III: RADIAL EMITTANCE AREA

Arc Current = 1 amp
Energy = 30 keV

Chimney Type*	Emittance Area for 100% Current		Emittance Area for ~95% Current	
	Area mm-mrad	Current mA	Area mm-mrad	% Current
0° L	370	4.24	207	90
0° S	312	3.22	216	95
10° L	293	1.67	196	96
10° S	293	1.93	195	95
20° L	194	1.25	146	97

TABLE IV: RADIAL EMITTANCE AREA

Arc Current = 5 amps
Energy = 30 keV

Chimney Type*	Emittance Area for 100% Current		Emittance Area for ~90% Current	
	Area mm-mrad	Current mA	Area mm-mrad	% Current
0° L	525	9.88	309	84
0° S	404	12.74	224	93
10° L	478	6.06	262	92
10° S	436	7.99	215	90
20° L	307	5.55	183	91

TABLE V: LUMINOSITY

Energy = 30 keV

Chimney Type*	Luminosity at 1 amp arc current ~ 85% total current amps/cm²-sr	Luminosity at 5 amps arc current ~85% total current amps/cm²-sr
0° L	22.2	33.5
0° S	18.3	48.3
10° L	11.6	23.9
10° S	15.2	40.7
20° L	12.2	33.2

* Degrees are the amount of recesses of chimney face. S means barrel diameter of 0.500"; L means barrel diameter of 0.720".

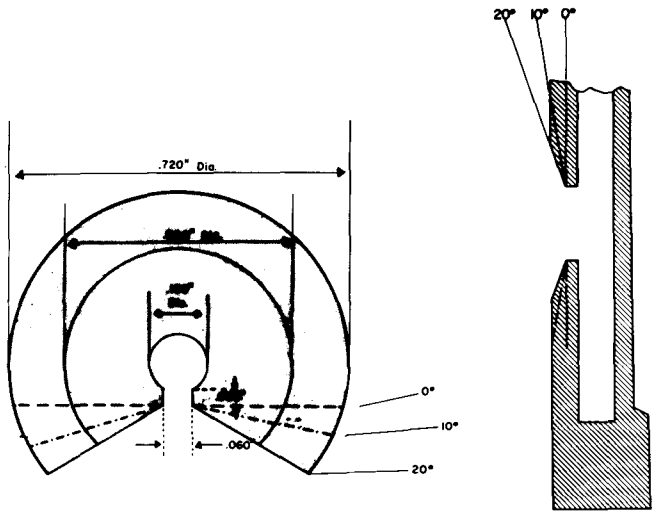

Fig. 1. Drawing of median plane (left) and vertical (right) cross section of a cyclotron ion source chimney indicating the different chimney geometrical variations.

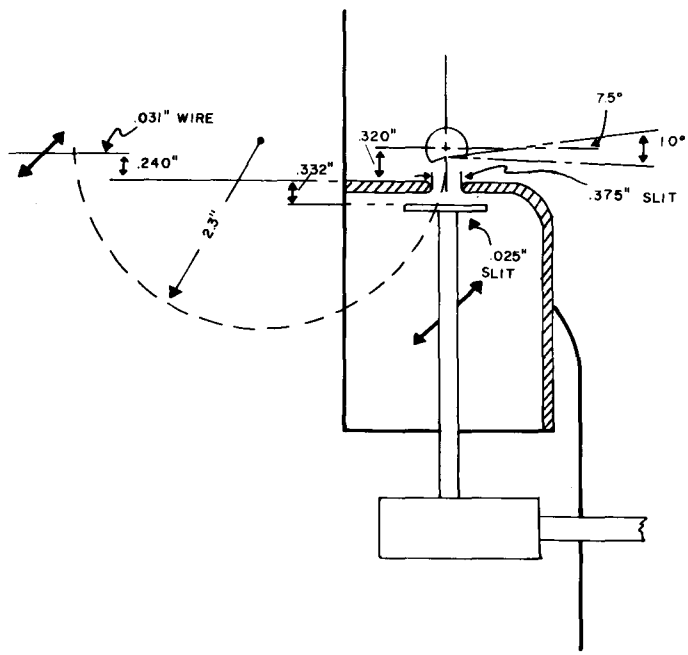

Fig. 2. Median plane view of axial emittance area probes. The chimney is located at the upper right, and the dashed line indicates an ion beam. The axial position slit is licated directly behind the puller and the axial angular divergence differential current probe is located at 180° beam position.

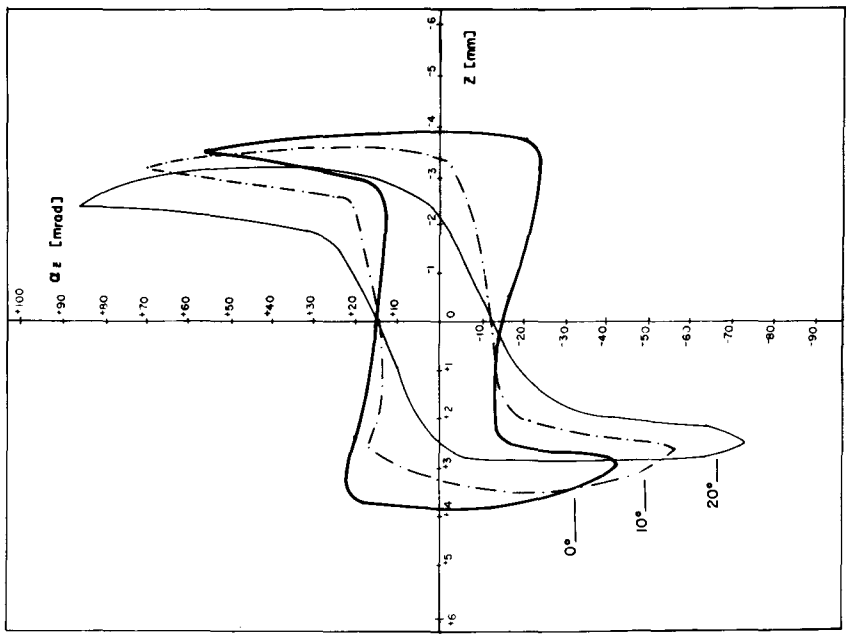

Fig. 4. The measured axial emmitance area for a 0°, 10° and 20° chimneys showing the rotation of the emittance areas about zero angular divergence.

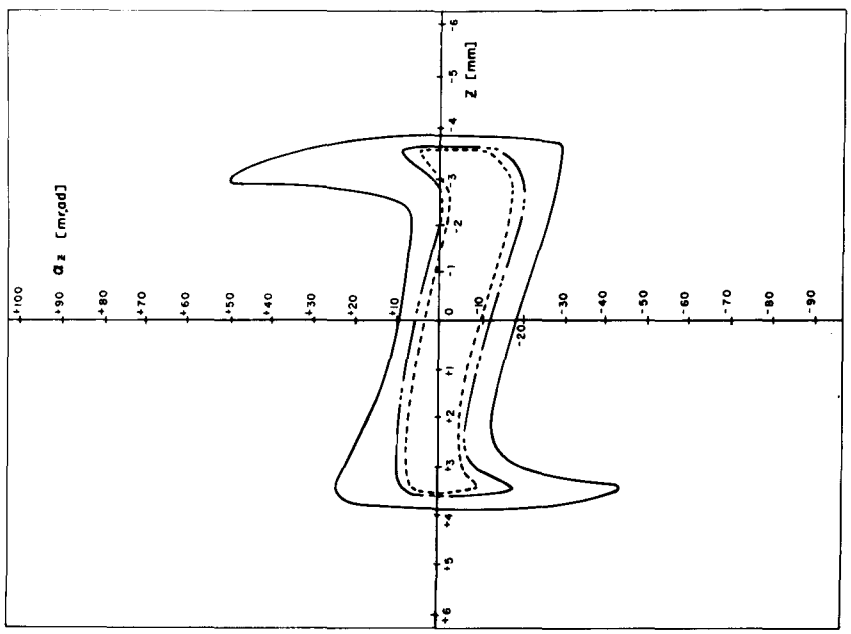

Fig. 3. The measured axial emittance area for a 0° (L) chimney at 1 amp arc current. The outer solid line is the 100% current (4.24 mA) emittance area and is 278 mm-mrad. The dashed lines are density contours obtained for 87.5% and 77.0% of the beam current and are 126 and 90 mm-mrad, respectively.

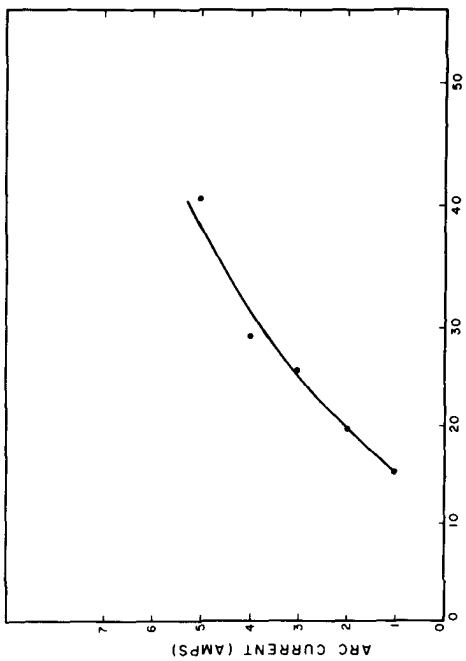

Fig. 6. The calculated luminosity for 10° (S) chimney as a function of arc current.

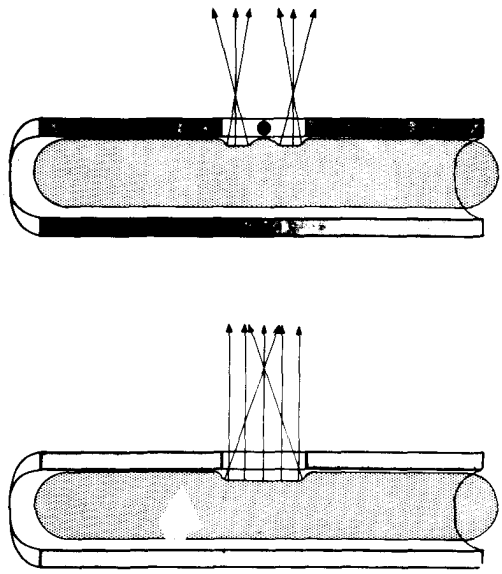

Fig. 7. Drawings of the vertical cross section of the chimney with the light dotted areas representing the plasma. On the left side the plasma is shown concave and direction of ions emitted from the surface are indicated by the arrows (angle exaggerated). The right side shows the plasma froming two concave surfaces with a 0.031" diameter wire inserted in the center of the chimney slit.

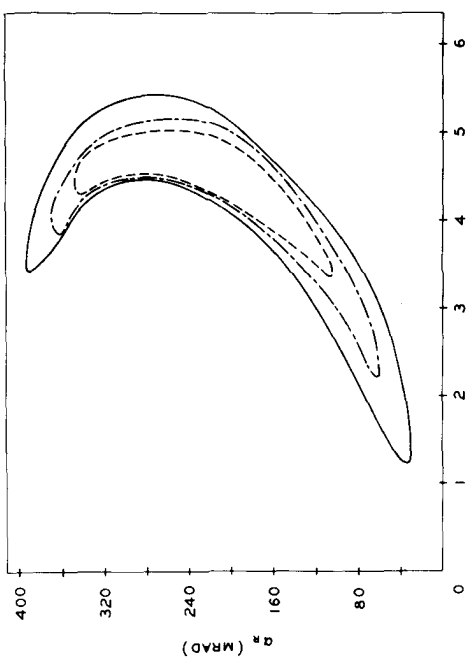

Fig. 5. The measured radial emittance area for a 0° (L) chimney at 1 amp arc current. The outer solid line is the 100% current (4.24 mA) emittance area and is 370 mm-mrad. The dashed lines are density contours obtained for 90% and 70% of the beam current and are 206 and 131 mm-mrad, respectively.

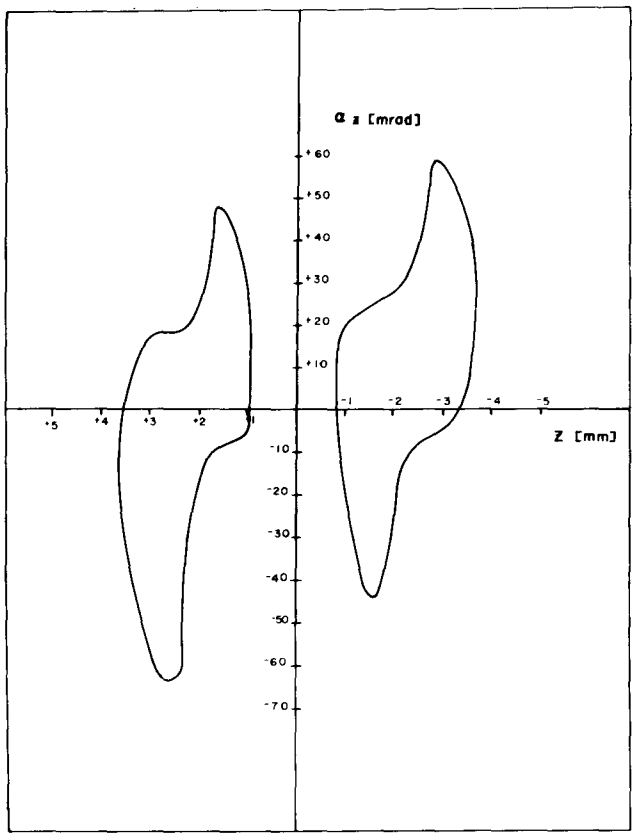

Fig. 8. The axial emittance area obtained for a chimney with a 0.031" diameter wire inserted in the center of the chimney slit.

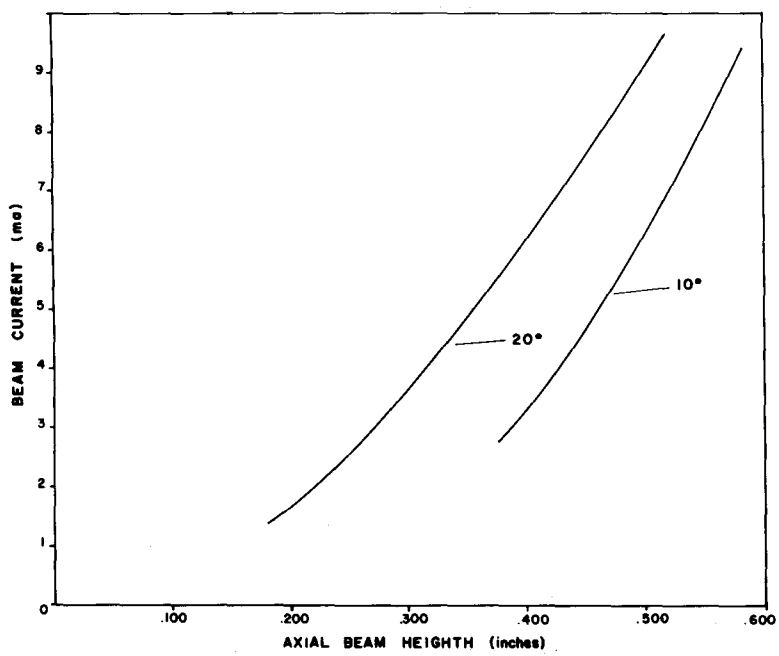

Fig. 9. The axial beam height (at 180° beam position measured as a function of total current for a 10° and 20° chimney.

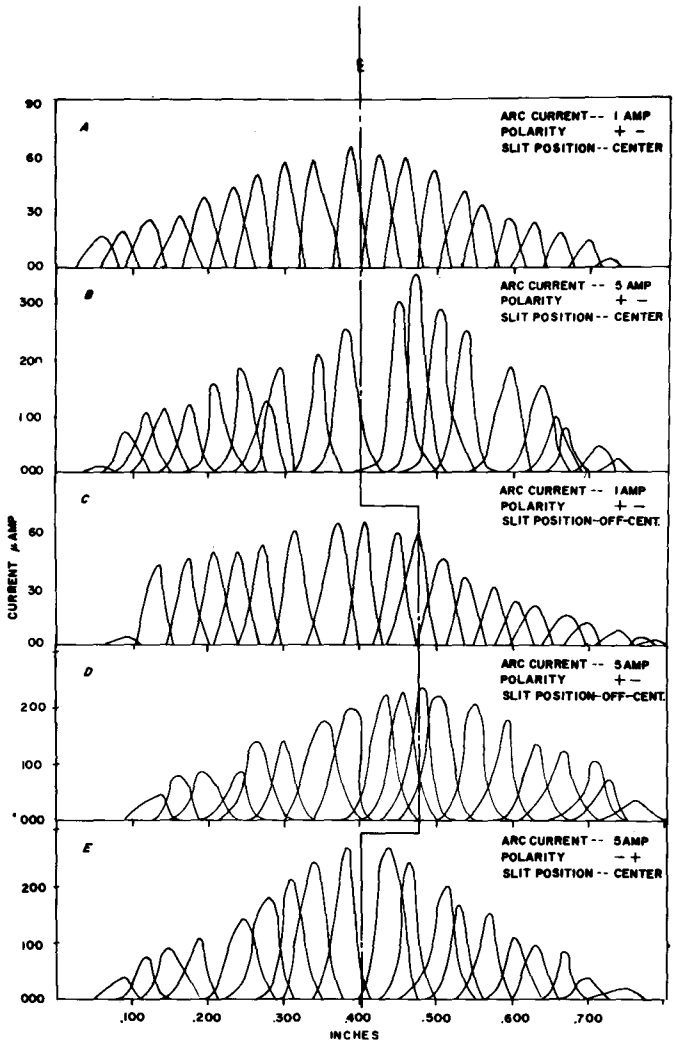

Fig. 10. Measurements of the radial an angular divergence for different radial slit positions as a function of arc current (a) and (b). For a chimney slit shifted 0.010 (c) and (d); and for reversed filament current (e). ℄ indicates center of beam.

DISCUSSION

BLOSSER: I would like to call attention to the fact that all the axial and radial emittance figures are at 30 keV energy. If one corrects them up to say 50 MeV, which is a usual measuring place, they come down to be less than 10 mm-mrad, indicating that the cyclotron source, as it is normally used, is an extremely fine source.

WEGNER: It has been my observation that, when the rf comes on in the cyclotron, the rf field from the port seems to affect the plasma in the chimney. You can actually see it snap back inside. There is also some evidence that test bench results with this type of source don't always agree with the performance in the machine. Do these results come out the same on your machine as they do on the test bench?

BLOSSER: You expect the plasma boundary to be shifted by the extraction field; the results are completely consistent with what one observes in the machine. One does not have sufficient information to make very detailed comparisons, but there is no inconsistency.

REISER: Did you measure the fraction of molecular ions in your beams?

MALLORY: We observed but didn't measure them.

REISER: Perhaps the shifting of your intensity maximum could also be explained by a change in the fractions of H_2^+ and H_3^+ when the arc conditions changed.

MALLORY: Agreed. There are other things that can change in the ion source. For instance, Livingston and Jones have noticed that with a change in the width of the chimney slit, or a change in the diameter of the plasma column, these results may be varied.